

## Diffusion-weighted magnetic resonance imaging for monitoring prostate cancer progression in patients managed by active surveillance

<sup>1</sup>V A MORGAN, MSc, <sup>1</sup>S F RICHES, MSc, <sup>2</sup>K THOMAS, MSc, <sup>3</sup>N VANAS, MRCP, FRCR, <sup>3</sup>C PARKER, MD, FRCR, <sup>1</sup>S GILES, BSc and <sup>1</sup>N M DESOUZA, MD, FRCR

<sup>1</sup>Cancer Research UK Clinical Magnetic Resonance Research Group, <sup>2</sup>Department of Statistics, and <sup>3</sup>Academic Urology Unit, Institute of Cancer Research and Royal Marsden NHS Foundation Trust, Downs Road, Sutton SM2 5PT, UK

**Objectives:** We studied patients managed by active surveillance to determine whether there was a difference over time in apparent diffusion coefficients (ADCs) derived from diffusion-weighted MRI in those who progressed to radical treatment (progressors,  $n=17$ ) compared with those who did not (non-progressors,  $n=33$ ).

**Methods:** 50 consecutive patients (Stage T1/2a, Gleason grade  $\leq 3+4$ , prostate-specific antigen (PSA)  $<15$  ng ml<sup>-1</sup>,  $<50\%$  cores positive) were imaged endorectally (baseline and 1–3 years follow-up) with  $T_2$  weighted ( $T_2W$ ) and echo-planar diffusion-weighted MRI sequences. Regions of interest drawn on ADC maps with reference to the  $T_2W$  images yielded ADC<sub>all</sub> ( $b=0$ –800), ADC<sub>fast</sub> ( $b=0$ –300) and ADC<sub>slow</sub> ( $b=300$ –800) for whole prostate (minus tumour) and tumour (low signal-intensity peripheral zone lesion in biopsy-positive octant).

**Results:** Tumour and whole prostate ADC<sub>all</sub> and ADC<sub>fast</sub> were significantly reduced over time in progressors ( $p=0.03$  and  $0.03$  for tumours, respectively;  $p=0.02$  and  $0.007$  for the whole prostate, respectively). There were no significant changes in ADC over time in non-progressors. A 10% reduction in tumour ADC<sub>all</sub> indicated progression with a 93% sensitivity and 40% specificity ( $A_z$  of receiver operating characteristic (ROC) curve = 0.68). Percentage reductions in whole prostate ADC<sub>all</sub>, ADC<sub>fast</sub> and ADC<sub>slow</sub> were also significantly greater in progressors than in non-progressors ( $p=0.01$ ,  $0.03$  and  $0.008$ , respectively).

**Conclusion:** This pilot study shows that DW-MRI has potential for monitoring patients with early prostate cancer who opt for active surveillance.

Received 27 October 2009  
Revised 8 December 2009  
Accepted 16 December 2009

DOI: 10.1259/bjr/14556365

© 2011 The British Institute of Radiology

Patients with early-stage prostate cancer may be offered active surveillance because of the indolent nature of the disease in many cases. This involves regular monitoring with prostate-specific antigen (PSA) levels and repeat biopsy. Repeat biopsy is invasive, sometimes poorly tolerated and carries a risk of morbidity. Non-invasive imaging methods are therefore being explored increasingly to provide biomarkers of prostate cancer behaviour.

Although  $T_2$  weighted ( $T_2W$ ) MRI is the best way of visualising anatomical detail within the prostate, it has a sensitivity of just 60–76% for disease detection within the gland, with a specificity of around 55% [1, 2]. An increasingly useful addition to conventional  $T_2W$  MRI is the use of “apparent diffusivity” (tissue water incoherent displacement over distances of 1–20  $\mu\text{m}$ ) to develop image contrast. Diffusion-weighted (DW) MRI has been used in both clinical and research settings to detect and evaluate a variety of tumour types [3–7]. In prostate cancer, DW-MRI is proving useful in tumour detection [8]. The apparent diffusion coefficients

(ADCs) that are derived by this technique provide quantitative information on the degree to which water diffusion, including the contributions made by microcapillary perfusion and true diffusion within the extracellular space, is restricted within tissues. ADCs are therefore directly associated with coherent microvessel density and cellularity [9] and with microcapillary perfusion (which contribute to a “fast” diffusion component), and with water movement within the extracellular or intracellular space over a shorter diffusion path (which contributes to a “slow” diffusion component). We have shown previously that significant differences in tumour ADCs exist between patients with low-risk and higher-risk localised prostate cancer, and that this is the case for both the fast and the slow components [10]. Changes in ADC components in the tumour and in the surrounding normal prostate tissue have not, however, been studied previously in relation to disease progression in low-risk patients managed by active surveillance. The aim of this pilot study of patients managed by active surveillance was therefore to use DW-MRI to establish whether the changes in tumour and whole prostate ADCs in patients who progressed to radical treatment differed over time from those in patients whose disease did not progress.

Address correspondence to: Profesor N M deSouza, MRI Unit, Royal Marsden Hospital, Downs Road, Sutton, Surrey SM2 5PT, UK. E-mail: nandita.desouza@icr.ac.uk

## Methods and materials

### Patient population

This was a single-institution, longitudinal, retrospective pilot study with institutional approval from the local research ethics committee. The study included 50 consecutive patients with localised prostate cancer (Stage T1 or 2a disease; Gleason 3+3 ( $n=41$ ), 3+4 ( $n=8$ ), 4+3 ( $n=1$ ); median PSA 7.2 ng ml<sup>-1</sup> (minimum 0.4 ng ml<sup>-1</sup>, maximum 15.0 ng ml<sup>-1</sup>); <50% cores positive) who had had MRI for clinical staging within 4 months of diagnostic biopsy and who had opted for management within an active surveillance research programme. Patients underwent DW-MRI in addition to their standard T<sub>2</sub>W MRI at baseline (time-point 1). All patients had a follow-up MRI as part of the active surveillance monitoring schedule (time-point 2) after a mean of 24 months (median 24 months, minimum 7 months, maximum 41 months). The patients were classified at the time of this second MRI as non-progressors (who continued on active surveillance) or as progressors to radical treatment (those requiring treatment within 6 months). The time between baseline and follow-up scan was not significantly different in non-progressors compared with progressors (25 ± 7 months for non-progressors; 23 ± 8 months for progressors). All untreated patients had at least 12 months of follow-up. Radical treatment was recommended to patients with a PSA velocity >1 ng ml<sup>-1</sup> per year or with adverse features on repeat biopsy (defined as Gleason score >3+4 or >50% of cores involved) [11]. The clinicians responsible for treatment (CP and NVA) were blinded to the MRI results.

### MRI data acquisition

MR studies were done on a 1.5T Intera system (Philips Medical Systems, the Netherlands) using a balloon design endorectal coil (Philips Medical Systems) inflated with 55 ml of air. Hyoscine butyl bromide (20 mg) was administered intramuscularly immediately prior to centring the patient in the scanner in order to reduce peristalsis: this is routine at our institution for abdominopelvic MRI and this drug is preferred to glucagon because it provides more effective antiperistalsis. None of our patients had a history of urinary retention. Hyoscine butyl bromide is contraindicated in patients with large prostates and urinary retention, but when given intramuscularly at this dose, we have had no cases of urinary retention in >500 prostate examinations. Conventional T<sub>2</sub>W fast-spin-echo images were obtained in three orthogonal planes (turbo spin echo (TSE) 2000/90 ms (repetition time (TR)/effective time to echo (TE), echo train length 16, 2 signal averages) with a 256 × 512 matrix re-sampled to 512 × 512, 3 mm slice thickness, no gap and a 14 cm field of view (FOV) (total imaging time 12 min). Echo-planar DW images (DWI 2500/69 ms (TR/TE)) with  $b$ -values of 0, 300, 500 and 800 s/mm<sup>2</sup> were obtained transverse to the prostate and parallel to the corresponding set of T<sub>2</sub>W images. The phase-encoding gradient was from left to right in order to minimise motion artefacts in the prostate. Either 12 or 18 3–4 mm thick slices (no gap, 20 cm FOV, matrix 128) provided coverage of the prostate with an image acquisition time of 1 min 40 s. ADC maps were generated using the system software and all  $b$ -values.

Following endorectal MRI, an external pelvic phased array coil was used to acquire axial T<sub>1</sub> weighted (T<sub>1</sub>W) (TSE 650/7 ms (TR/TE) and T<sub>2</sub>W (TSE 5396/80 ms (TR/effective TE)) images through the pelvis as part of the routine clinical staging scan. The B<sub>0</sub> maps and T<sub>1</sub>W images confirmed the absence of any significant post-biopsy haemorrhage in this patient cohort.

### Data analysis

Axial T<sub>2</sub>W and DW-MRI images and ADC maps were transferred offline for analysis. Regions of interest (ROIs) were drawn around the whole prostate (peripheral zone and central gland) and around the tumour (low-signal-intensity lesion in a sextant biopsy positive for tumour) on the scanner-generated ADC maps. As the results were quantitative, the ROI placement was done by a single observer with 10 years' experience of prostate MRI. Mean ADC values ( $\times 10^{-3}$  mm<sup>2</sup> s<sup>-1</sup>) from tumour and whole prostate (minus tumour) regions were calculated from the ADC-derived ROIs using a weighted mono-exponential model that included all  $b$ -values (ADC<sub>all</sub>) for both baseline and follow-up imaging (in-house software developed using Interactive Data Language IDL; RSI Ltd, Boulder, CO). In addition, data obtained using just the low (0–300) or high (300–800)  $b$ -values were also analysed separately to reflect fast (ADC<sub>fast</sub>) and slow (ADC<sub>slow</sub>) diffusion components [12]. Values for ADC<sub>all</sub>, ADC<sub>fast</sub> and ADC<sub>slow</sub> were calculated in patients who progressed to radical treatment ( $n=17$ ) and compared with values from those that did not ( $n=33$ ).

### Statistical analysis

Statistical analysis of the data was performed using SPSS, version 15.0 (Chicago, IL) for Windows. ADC data for whole prostate and tumour at both time points were tested for normality using a Shapiro–Francia normality test. All data were normally distributed. ADC values for the tumour and whole prostate (minus tumour) regions were compared between time-points 1 (baseline) and 2 (follow-up) using paired  $t$ -tests. Means and standard deviations of the absolute change and mean percentage changes were calculated for the whole group. Percentage ADC changes in patients who progressed to radical treatment were compared with those in patients who continued on active surveillance after time-point 2 using an unpaired  $t$ -test (unequal variance assumed). All significance tests were two-sided and a  $p$ -value of <0.05 was chosen as the criterion for statistical significance. A receiver operating characteristic (ROC) curve was used to determine the sensitivity and specificity of a cut-off value for change in a parameter for indicating progression to radical treatment.

## Results

### Changes in tumour and gland volumes

In non-progressors, tumour and whole gland volumes (mean ± SD) determined from ROI sizes were 0.33 ± 0.38 cm<sup>3</sup> and 53.7 ± 27.0 cm<sup>3</sup>, respectively, at

time-point 1 and  $0.47 \pm 0.45 \text{ cm}^3$  and  $59.4 \pm 31.1 \text{ cm}^3$ , respectively, at time-point 2. In progressors, these data were  $1.1 \pm 1.9 \text{ cm}^3$  and  $44.6 \pm 17.8 \text{ cm}^3$ , respectively, at time-point 1 and  $1.1 \pm 1.2 \text{ cm}^3$  and  $46.0 \pm 21.1 \text{ cm}^3$ , respectively, at time-point 2. PSA concentrations rose from  $6.4 \pm 3.6 \text{ ng ml}^{-1}$  at time-point 1 to  $7.9 \pm 4.6 \text{ ng ml}^{-1}$  at time-point 2 in non-progressors, compared with a rise from  $8.4 \pm 2.4 \text{ ng ml}^{-1}$  to  $10.8 \pm 3.8 \text{ ng ml}^{-1}$  in progressors. There was no significant change over time in tumour or whole gland volume in either group. The change in PSA concentration over time approached significance ( $p=0.059$ ), which is to be expected as this parameter is used as a criterion for defining progression.

No tumour was visible in 7 of the 33 non-progressors and in 1 of the 17 progressors. Tumour ADC values were therefore obtained from 26 non-progressors and 16 progressors, whereas whole prostate ADC values were obtained from the entire cohort. Table 1 shows the mean  $\text{ADC}_{\text{all}}$ ,  $\text{ADC}_{\text{fast}}$  and  $\text{ADC}_{\text{slow}}$  values for the entire patient cohort, for those that did not progress to radical treatment (non-progressors) and for those that did (progressors). Representative  $T_2W$  images with corresponding ADC maps from a non-progressor and a progressor are illustrated in Figures 1 and 2, respectively. When tumour regions for the entire cohort were considered together,  $\text{ADC}_{\text{all}}$  and  $\text{ADC}_{\text{fast}}$  were significantly lower at time-point 2 than at time-point 1, but there was no significant change over time in  $\text{ADC}_{\text{slow}}$  (Table 1). This may be explained by the inherently lower signal to noise ratio (SNR), and thus greater variability of the data, at higher  $b$ -values. Differences in whole prostate ADC values between the time-points were not significant.

At the outset (time-point 1), the  $\text{ADC}_{\text{all}}$ ,  $\text{ADC}_{\text{fast}}$  and  $\text{ADC}_{\text{slow}}$  in progressors were not significantly different from those in non-progressors. When data from the non-progressors and progressors were analysed separately, it was evident however that the significant reduction in tumour  $\text{ADC}_{\text{all}}$  and  $\text{ADC}_{\text{fast}}$  seen over time could be

attributed to the progressors ( $p=0.03$ ) because there was no significant change in these components in non-progressors. The whole prostate also showed a significant reduction in  $\text{ADC}_{\text{all}}$  ( $p=0.02$ ) and  $\text{ADC}_{\text{fast}}$  ( $p=0.007$ ) in progressors but not in non-progressors, indicating reduced microcapillary perfusion over both the tumour and the whole prostate over time in the progressors. When comparing percentage change in  $\text{ADC}_{\text{all}}$ ,  $\text{ADC}_{\text{fast}}$  and  $\text{ADC}_{\text{slow}}$  in non-progressors and progressors, all whole prostate ADC values were significantly lower in progressors than in non-progressors (Figure 3a, Table 2). Tumour ADC values were not significantly different, however, possibly because of high variability between patients (Figure 3b). ROC curve analysis showed an area under curve of 0.68 for change in tumour  $\text{ADC}_{\text{all}}$ . A 10% reduction in tumour ADC predicted progression with a 93% sensitivity and 40% specificity. For  $\text{ADC}_{\text{fast}}$ , a 10% reduction in value predicted progression with a 66.7% sensitivity and 40% specificity ( $A_z=0.45$ ); for  $\text{ADC}_{\text{slow}}$ , a 10% reduction in value predicted progression with a 66.7% sensitivity and 36% specificity ( $A_z=0.46$ ).

### Discussion

This pilot study showed that ADC values for both tumours and whole prostate were significantly reduced at follow-up in patients who progressed to radical treatment, although the reduction in  $\text{ADC}_{\text{slow}}$  was not significant, possibly because of low SNR and relatively high variability between patients. Although it was not possible to "test reproducibility" by including a second baseline measurement, the stability of values for whole prostate  $\text{ADC}_{\text{all}}$  in non-progressors across the two time-points indicates that this measurement is reproducible. The reduction over time in tumour and whole prostate  $\text{ADC}_{\text{fast}}$  in progressors was unexpected and indicates a reduction in microcapillary perfusion within both the

**Table 1.** Comparison of ADC components with time for whole prostate and tumour regions over the entire cohort and in the subsets of those who progressed to radical treatment and those who did not

	$\text{ADC}_{\text{all}}$		$\text{ADC}_{\text{fast}}$		$\text{ADC}_{\text{slow}}$	
	WP mean $\pm$ SD $\times 10^{-3}$	*Tumour mean $\pm$ SD $\times 10^{-3}$	WP mean $\pm$ SD $\times 10^{-3}$	*Tumour mean $\pm$ SD $\times 10^{-3}$	WP mean $\pm$ SD $\times 10^{-3}$	*Tumour mean $\pm$ SD $\times 10^{-3}$
Whole group TP1	$1.73 \pm 0.14$	$1.43 \pm 0.29$	$1.99 \pm 0.16$	$1.62 \pm 0.32$	$1.35 \pm 0.10$	$1.16 \pm 0.24$
Whole group TP2	$1.74 \pm 0.10$	$1.34 \pm 0.24$	$1.94 \pm 0.11$	$1.52 \pm 0.26$	$1.35 \pm 0.10$	$1.11 \pm 0.21$
$p$ -value (TP1 vs TP2)	0.35	<b>0.06</b>	0.11	<b>0.049</b>	0.72	0.3
Progressors TP1	$1.76 \pm 0.10$	$1.33 \pm 0.20$	$2.03 \pm 0.113$	$1.53 \pm 0.23$	$1.37 \pm 0.09$	$1.08 \pm 0.18$
Progressors TP2	$1.684 \pm 0.08$	$1.20 \pm 0.13$	$1.92 \pm 0.09$	$1.37 \pm 0.17$	$1.33 \pm 0.08$	$1.00 \pm 0.12$
$p$ -value (TP1 vs TP2)	<b>0.02</b>	<b>0.03</b>	<b>0.007</b>	<b>0.03</b>	0.18	0.16
Non-progressors TP1	$1.72 \pm 0.16$	$1.49 \pm 0.33$	$1.97 \pm 0.18$	$1.68 \pm 0.36$	$1.34 \pm 0.10$	$1.21 \pm 0.25$
Non-progressors TP2	$1.72 \pm 0.12$	$1.41 \pm 0.26$	$1.96 \pm 0.12$	$1.60 \pm 0.26$	$1.37 \pm 0.11$	$1.17 \pm 0.23$
$p$ -value (TP1 vs TP2)	0.92	0.36	0.72	0.37	0.23	0.54

\*Tumour values for  $n=26$  non-progressors and  $n=16$  progressors in whom a tumour was visible. Whole prostate (WP) values are given for the entire cohort. TP, time-point. ADC, apparent diffusion coefficient.

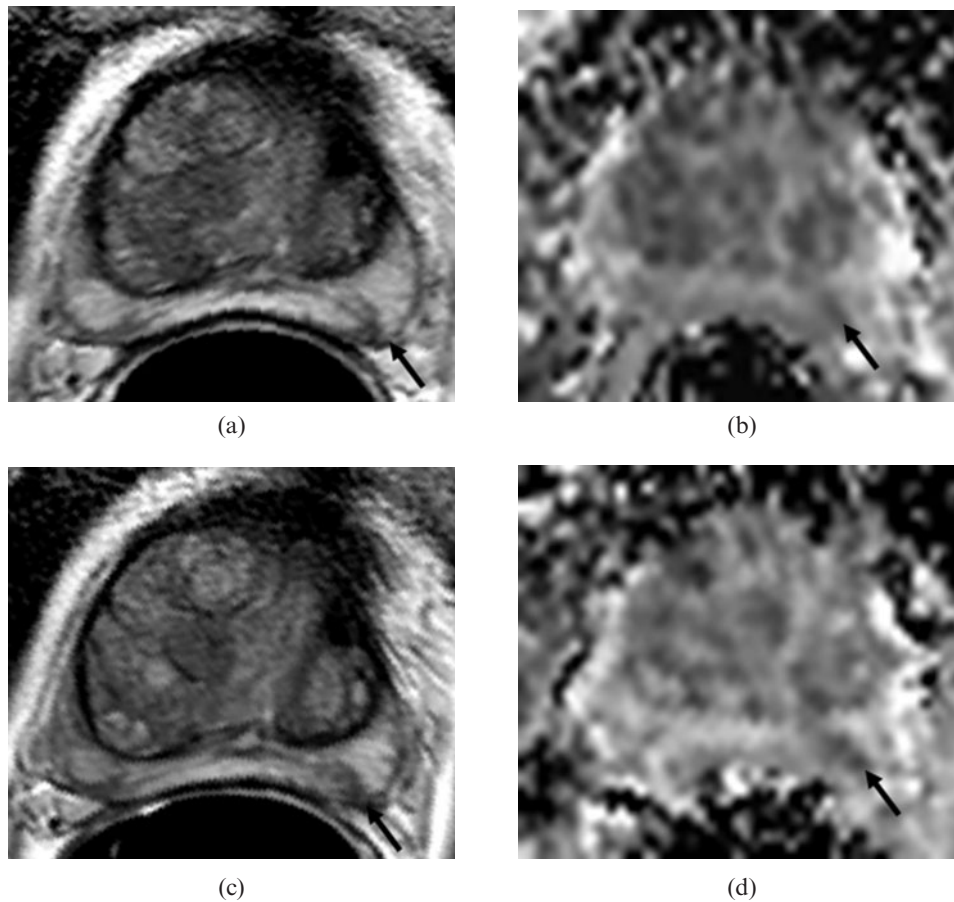


**Figure 1.** Non-progressor to radical treatment showing tumour in the left midzone of the prostate (arrows) at baseline on (a)  $T_2W$  ( $T_2$  weighted) axial (turbo spin-echo 2000/90 ms (repetition time (TR)/effective time to echo (TE), echo train length 16) and (b) the corresponding apparent diffusion coefficient (ADC) map (echo planar single shot diffusion-weighted image 2500/69 ms (TR/TE),  $b$ -values of 0, 300, 500 and 800  $\text{s mm}^{-2}$ ) and after 24 months of follow-up on (c)  $T_2W$  axial and (d) the corresponding ADC map. No change in appearance between the two time-points is seen.

tumour and the whole gland over a period of 2–3 years. Previous studies that have used colour Doppler ultrasound to map the vascular anatomy of the prostate have demonstrated hypervascularisation of the peripheral zone of patients with prostate cancer [13, 14]. Conversely, hypoxia is known to promote proliferation of prostate stromal cells in culture, and when measured invasively using a polarographic electrode has also been found to be a feature of prostate cancer [15]. To our knowledge, however, a reduction in vascularity within non-tumour regions of the prostate over time has not been described previously. It may be that this factor is an important driver of disease progression, and this is supported by *ex vivo* findings of increased hypoxia in more aggressive tumour types [16]. A larger series using dynamic contrast-enhanced MRI to compare modelled vascular parameters of perfusion and permeability in patients on active surveillance programmes would be useful.

The mean area for a tumour ROI in this study, measured on both the  $T_2W$  images and the ADC maps, was  $\sim 20 \text{ mm}^2$ . Pixel sizes of  $0.27 \times 0.27 \text{ mm}$  on  $T_2W$  images and  $1.6 \times 1.6 \text{ mm}$  on the ADC maps meant that, on average, each tumour ROI encompassed  $\sim 274$  pixels on a  $T_2W$  image slice *vs*  $\sim 8$  pixels on the ADC maps. Partial volume effects from tissue adjacent to the ADC-determined ROIs are therefore a significant problem. The image matrix size,

FOV and slice thickness were compromised in order to achieve a reasonable SNR within a reasonable timeframe that was clinically acceptable. Use of an external coil in conjunction with an endorectal coil or an endocavitary array would improve SNR and provide DW-MRI of greater spatial resolution and reduced partial volume effects when assessing small tumours within same timeframe.

The  $b$ -values chosen for our study enabled discrimination of fast and slow diffusion components. Although some researchers have advocated the use of  $b$ -values of  $1000 \text{ s mm}^{-2}$  to separate out the slow diffusion components adequately [17], our data show that values up to  $800 \text{ s mm}^{-2}$  are sufficient: use of higher  $b$ -values merely serves to increase the noise in the acquired data. *Ex vivo* data show that it is the slow diffusion component that is associated with cell density [18]. Thus, the ADC differences that discriminate progressors to radical treatment *vs* non-progressors are expected to be due to more dense cellular regions in the former group. An improvement in SNR would, however, be required to detect this.

For DW-MRI of the prostate, single-shot echo-planar (EPI) sequences are favoured over TSE sequences because of the need to freeze bulk motion. However, the susceptibility-induced distortion to which single-shot EPI is prone can be problematic in prostate imaging where air in the rectum or within the balloon of

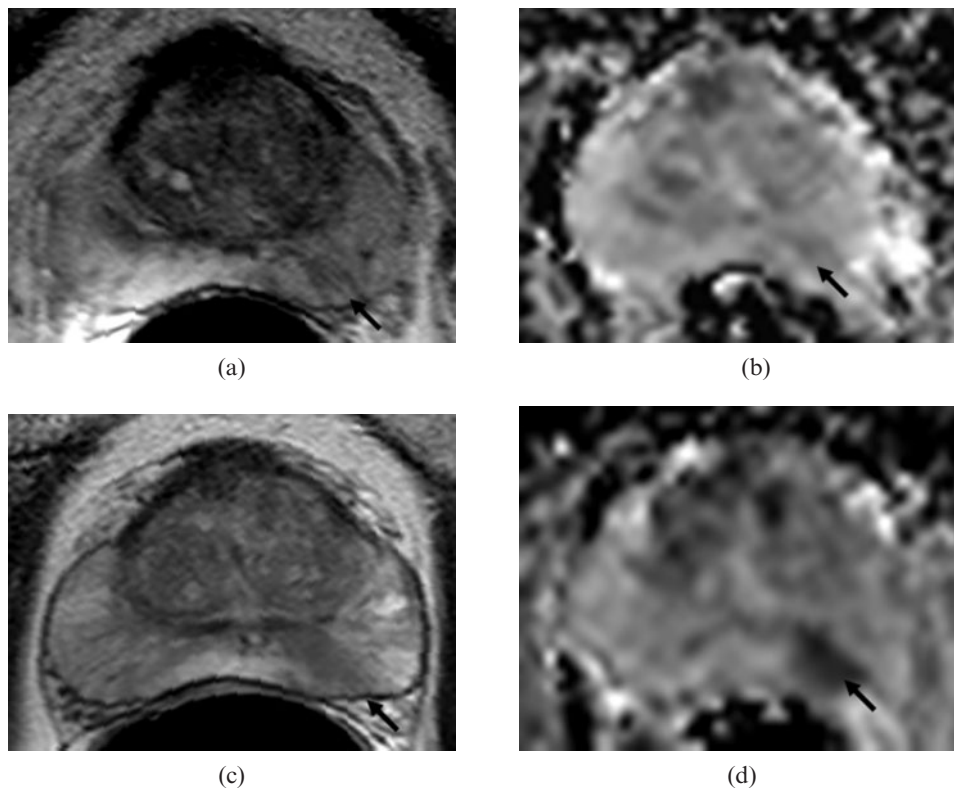


**Figure 2.** Images from a progressor to radical treatment showing tumour in the left mid-zone of the prostate (arrows) at baseline on (a)  $T_2W$  ( $T_2$  weighted) axial (turbo spin-echo 2000/90 ms (repetition time (TR)/effective time to echo (TE), echo train length 16) and (b) the corresponding apparent diffusion coefficient (ADC) map (echo planar single shot diffusion-weighted image 2500/69 ms (TR/TE),  $b$ -values of 0, 300, 500 and 800  $s\text{ mm}^{-2}$ ) and after 35 months of follow-up on (c)  $T_2W$  axial and (d) the corresponding ADC map. A change in the appearance of the tumour on the ADC maps between the two time-points is evident.

the endorectal coil causes significant local magnetic field inhomogeneity and susceptibility artefact. Our DWIs were acquired with an EPI readout and contained some distortion at tissue boundaries where there was a discontinuity in magnetic susceptibility. Advantages of an EPI sequence, however, are that it is possible to obtain

12 contiguous 4 mm-thick slices or 18 contiguous 3 mm slices, giving a supero-inferior coverage of 4.8 cm or 5.4 cm in less than 1.6 min. In all but two of our cases, this was sufficient to cover the prostate from apex to base.

Haemorrhage following biopsy can potentially alter ADC measurements. These effects can last for several

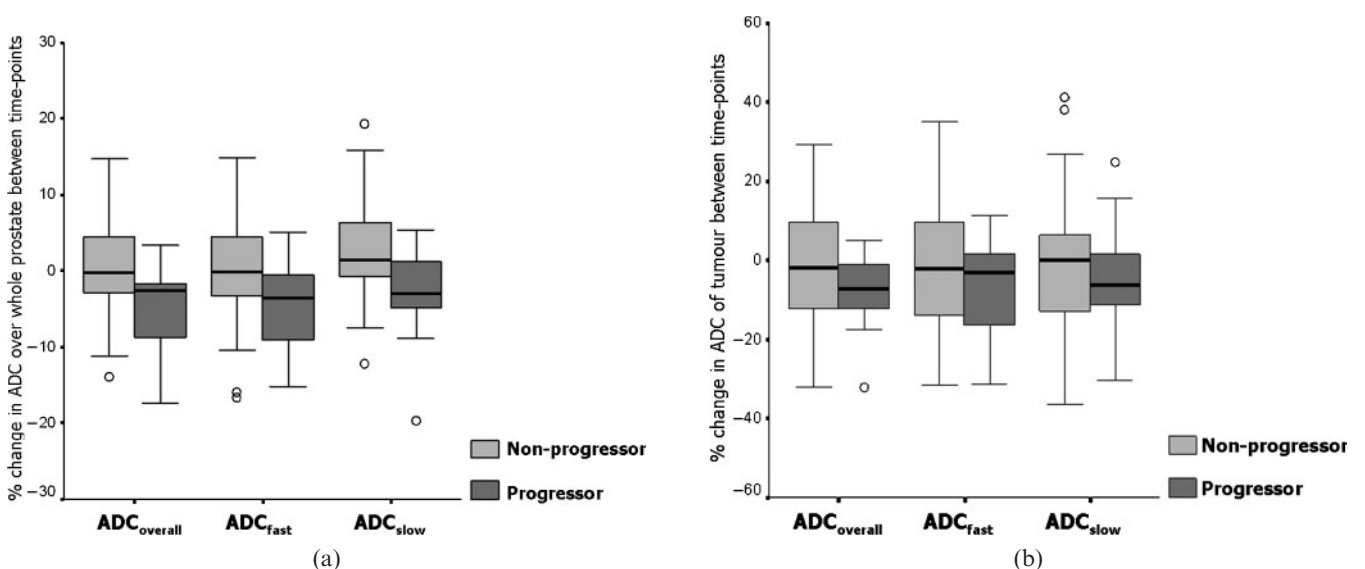


**Figure 3.** Percentage change in (a) whole prostate values and (b) tumour values for  $ADC_{all}$ ,  $ADC_{fast}$  and  $ADC_{slow}$  in progressors and non-progressors to radical treatment. Lower quartile, bottom line of box; median, middle line of box; upper quartile, top line of box; lower whisker, lower value; upper whisker, upper value; circles, outliers. ADC, apparent diffusion coefficient.

**Table 2.** Comparison of percentage change over time for those that progressed to radical treatment with those that did not

	ADC <sub>all</sub>		ADC <sub>fast</sub>		ADC <sub>slow</sub>	
	WP mean ±SD	Tumour mean ±SD	WP mean ±SD	Tumour mean ±SD	WP mean ±SD	Tumour mean ±SD
Progressor (n=11)	-4.1±5.4	-7.1±10.0	-4.8±5.9	-7.3±12.5	-2.7±5.8	-4.4±13.7
% change TP2-TP1						
Non-progressor (n=21)	0.6±6.5	-3.0±17.7	-0.3±7.0	-3.2±17.8	2.5±6.8	-1.2±19.4
% change TP2-TP1						
p-value	0.01	0.4	0.03	0.4	0.008	0.55

months, and time from biopsy to scan, even when done at the conventional 4 weeks post biopsy, may not be sufficient. In 11 cases, biopsy was performed for logistical reasons 3 weeks to 4 months before MRI at time-point 2. However, in none of these cases was there evidence of intraprostatic haemorrhage on the  $T_1W$  scans, nor was there any susceptibility artefact on the high  $b$ -value DWIs, indicating that the effects of haemorrhage on the ADC values were likely to be negligible.

In addition to the imaging limitations of poorer SNR when an external array is not used, ADC is affected by partial volume effects in the measurement of tumour regions and post-biopsy haemorrhage affecting ADC. This study is also limited by the definition of 'progressors', which must essentially be considered to be arbitrary because of the effects of sampling error on biopsy. The decision to institute radical treatment was based on the definitions of biochemical and histological disease progression, which are, of necessity, not evidence based. However, pre-treatment PSA velocity has been shown to be an important determinant of fatal prostate cancer in several different settings [19–21], and Gleason score is an established predictor of prostate cancer mortality in localised disease. The policy for this patient cohort was to do repeat biopsies at 2 years and for the MRIs to be done immediately before the repeat biopsies. Unfortunately, there was considerable variation in the timing of the repeat biopsies because of a mixture of clinical concern and patient compliance. A future study comparing ADC values in those that are selected for active surveillance and those that opt for radical treatment at outset should also prove interesting.

## Conclusion

This pilot study shows that DW-MRI has potential for monitoring patients with early prostate cancer who opt for active surveillance. The quantitative data obtained indicate that the ADCs of tumours are lower than those of the whole prostate, and that microcapillary perfusion both within a tumour and in the whole prostate reduces significantly with time in progressors to radical treatment; percentage reductions in microcapillary perfusion and true diffusion in the whole prostate also are significantly greater in progressors compared with non-progressors. This suggests that the identification of individual tumour regions is not of paramount importance in the development of ADC as a prognostic biomarker in prostate cancer patients managed with active surveillance. Further work in larger-scale studies is needed to support this finding.

## Acknowledgments

Supported by Cancer Research UK and the ESPRC Cancer Imaging Centre; in association with MRC, Department of Health (CUK C1060/A10334) and NHS funding to the NIHR Biomedical Research Centre.

## References

- Casciani E, Poletti E, Bertini L, Emiliozzi P, Amini M, Pansadoro V, et al. Prostate cancer: evaluation with endorectal MR imaging and three-dimensional proton MR spectroscopic imaging. *Radiol Med* 2004;108:530–41.
- Kirkham AP, Emberton M, Allen C. How good is MRI at detecting and characterising cancer within the prostate? *Eur Urol* 2006;50:1163–74.
- Chenevert TL, Stegman LD, Taylor JM, Robertson PL, Greenberg HS, Rehemtulla A, et al. Diffusion magnetic resonance imaging: an early surrogate marker of therapeutic efficacy in brain tumors. *J Natl Cancer Inst* 2000; 92:2029–36.
- Lo GG, Ai V, Chan JK, Li KW, Cheung PS, Wong TT, et al. Diffusion-weighted magnetic resonance imaging of breast lesions: first experiences at 3 T. *J Comput Assist Tomogr* 2009;33:63–9.
- Messiou C, Morgan VA, De Silva SS, Ind TE, deSouza NM. Diffusion weighted imaging of the uterus: regional ADC variation with oral contraceptive usage and comparison with cervical cancer. *Acta Radiol* 2009;50:696–701.
- Somford DM, Futterer JJ, Hambroek T, Barentsz JO. Diffusion and perfusion MR imaging of the prostate. *Magn Reson Imaging Clin N Am* 2008;16:685–95.
- Uto T, Takehara Y, Nakamura Y, Naito T, Hashimoto D, Inui N, et al. Higher sensitivity and specificity for diffusion-weighted imaging of malignant lung lesions without apparent diffusion coefficient quantification. *Radiology* 2009; 252:247–54.
- Shimofusa R, Fujimoto H, Akamata H, Motoori K, Yamamoto S, Ueda T, et al. Diffusion-weighted imaging of prostate cancer. *J Comput Assist Tomogr* 2005;29:149–53.
- Hayashida Y, Hirai T, Morishita S, Kitajima M, Murakami R, Korogi Y, et al. Diffusion-weighted imaging of metastatic brain tumors: comparison with histologic type and tumor cellularity. *AJNR Am J Neuroradiol* 2006;27:1419–25.
- deSouza NM, Riches SF, Vanas NJ, Morgan VA, Ashley SA, Fisher C, et al. Diffusion-weighted magnetic resonance imaging: a potential non-invasive marker of tumour aggressiveness in localized prostate cancer. *Clin Radiol* 2008;63: 774–82.
- van As NJ, deSouza NM, Riches SF, Morgan VA, Sohaib SA, Dearnaley DP, et al. A study of diffusion-weighted magnetic resonance imaging in men with untreated localised prostate cancer on active surveillance. *Eur Urol* 2008 [Epub ahead of print].
- Riches SF, Hawtin K, Charles-Edwards EM, deSouza NM. Diffusion-weighted imaging of the prostate and rectal wall: comparison of biexponential and monoexponential

- modelled diffusion and associated perfusion coefficients. *NMR Biomed* 2009;22:318–25.
13. Kelly IM, Lees WR, Rickards D. Prostate cancer and the role of color Doppler US. *Radiology* 1993;189:153–6.
  14. Rifkin MD, Sudakoff GS, Alexander AA. Prostate: techniques, results and potential applications of color Doppler US scanning. *Radiology* 1993;186:509–13.
  15. Parker C, Milosevic M, Toi A, Sweet J, Panzarella T, Bristow R, et al. Polarographic electrode study of tumor oxygenation in clinically localized prostate cancer. *Int J Radiat Oncol Biol Phys* 2004;58:750–7.
  16. Butterworth KT, McCarthy HO, Devlin A, Ming L, Robson T, McKeown SR, et al. Hypoxia selects for androgen independent LNCaP cells with a more malignant genotype. *Int J Cancer* 2008;123:760–8.
  17. Kitajima K, Kaji Y, Kuroda K, Sugimura K. High *b*-value diffusion-weighted imaging in normal and malignant peripheral zone tissue of the prostate: effect of signal-to-noise ratio. *Magn Reson Med Sci* 2008;7:93–9.
  18. Zehhof B, Pickles M, Liney G, Gibbs P, Rodrigues G, Kraus S, et al. Correlation of diffusion-weighted magnetic resonance data with cellularity in prostate cancer. *BJU Int* 2009;103:883–8.
  19. Carter HB, Ferrucci L, Kettermann A, Landis P, Wright EJ, Epstein JI, et al. Detection of life-threatening prostate cancer with prostate-specific antigen velocity during a window of curability. *J Natl Cancer Inst* 2006;98:1521–7.
  20. D'Amico AV, Chen MH, Roehl KA, Catalona WJ. Pre-operative PSA velocity and the risk of death from prostate cancer after radical prostatectomy. *N Engl J Med* 2004;351:125–35.
  21. D'Amico AV, Renshaw AA, Sussman B, Chen MH. Pretreatment PSA velocity and risk of death from prostate cancer following external beam radiation therapy. *JAMA* 2005;294:440–7.